The Abdus Salam
International Centre for Theoretical Physics

United Nations
Educational, Scientific and
Cultural Organization

IAEA
International Atomic Energy Agency

2145-1

Spring College on Computational Nanoscience

17 - 28 May 2010

Stability of metal nanoclusters - shells of atoms and electrons

Hannu HAKKINEN
Nanoscience Center, Dept. of Physics and Chemistry
University of Jyvaskyla
Finland

Stability of metal nanoclusters – shells of atoms and electrons

Hannu Häkkinen

Lecture 1

Trieste 5/2010

Cluster science – at the heart of ”Nano” !

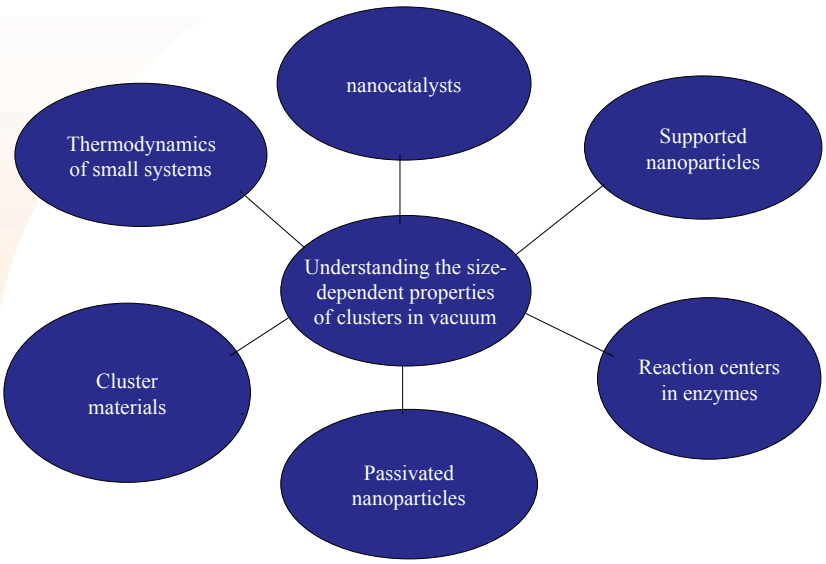

Some literature

- R. L. Johnston, Atomic and Molecular Clusters, Taylor & Francis (2002).
- W. A. de Heer, The physics of simple metal clusters: Experimental aspects and simple models, Rev. Mod. Phys **65**, 611 (1993).
- M. Brack, The physics of simple metal clusters: Self-consistent jellium model and semiclassical approaches, Rev. Mod. Phys. **65**, 677 (1993).
- F. Baletto, R. Ferrando, Structural properties of nanoclusters: Energetic, thermodynamic, and kinetic effects, Rev. Mod. Phys. **77**, 371 (2005).
- T. P. Martin, Shells of atoms, Phys. Rep. **273**, 199 (1996).
- L. D. Marks, Experimental studies of small particle structures, Rep. Prog. Phys. **57**, 603 (1994).

Manufacturing & analysis

Cluster sources

- Seeded supersonic nozzle source
- Gas-aggregation source
- Laser vaporization source
- Sputtering source
- Liquid-metal ion source

Cluster sources – overview

- Seeded supersonic nozzle source: intense continuous beams, low-boiling-point materials, evaporative cooling -> structured mass spectra (magic stabilities visible), temperature not well controlled
- Gas-aggregation cluster source: efficient for production of large clusters (up to 20 000+), low intensity, low-to-medium boiling point materials (< 2000 K), low cluster temperature (< 100 K)
- Laser vaporization source: pulsed beams from any material, cluster temperature near the source temperature
- Sputtering source: energetic heavy inert-gas ion sputtering beam (Kr+, Xe+, 10 – 20 keV) -> continuous beam of singly ionized (hot) clusters, cooling by evaporation
- Liquid-metal ion source: singly and multiply ionized (hot) clusters of low-melting point metals

Cluster sources

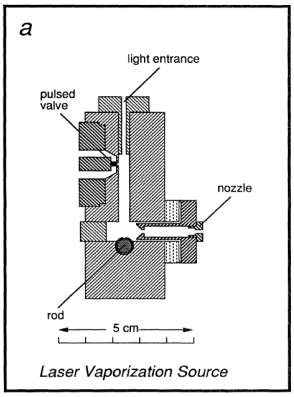

Laser Vaporization Source

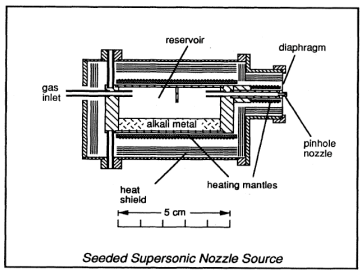

Seeded Supersonic Nozzle Source

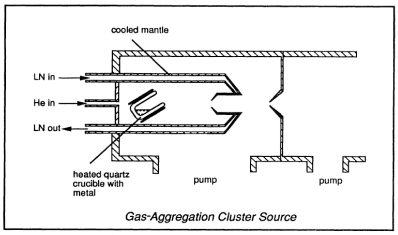

Gas-Aggregation Cluster Source

Cluster sources

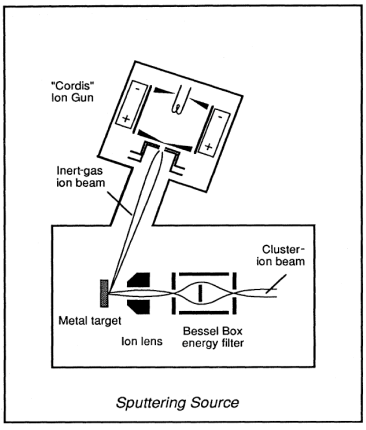

Sputtering Source

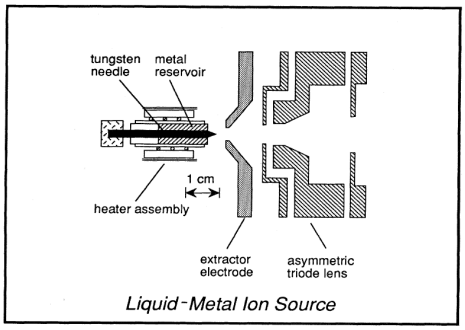

Liquid-Metal Ion Source

Analysis techniques

- Wien filter
- Quadrupole mass filter
- Time-of-flight mass spectrometry
- Ion cyclotron resonance mass spectrometry in ion trap
- Molecular-beam mobility analysis
- Electron diffraction in ion trap (structure factor)
- Photoelectron spectroscopy

Cluster mass analysis

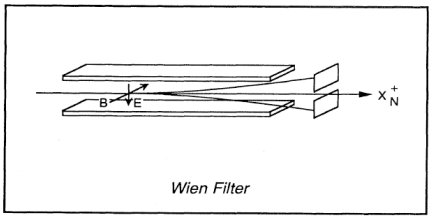

Wien Filter

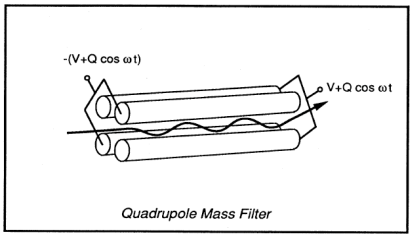

Quadrupole Mass Filter

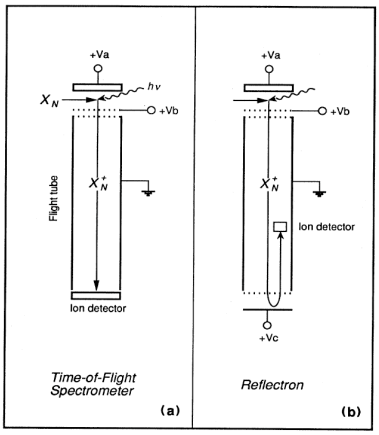

Example of a full setup

Gas-aggregation source

Photoionization by laser

Time-of-flight mass analysis

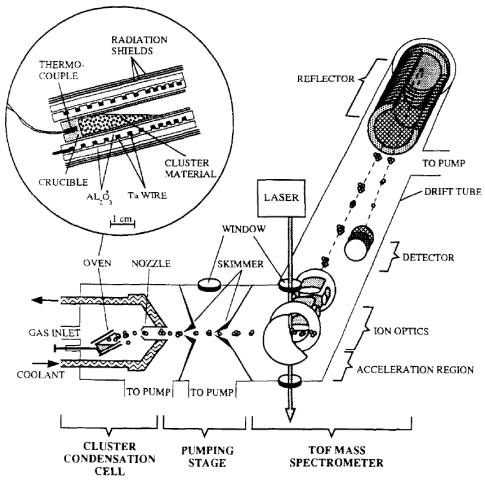

Martin, Phys. Rep. 273, 199 (1996)

Photoelectron spectroscopy

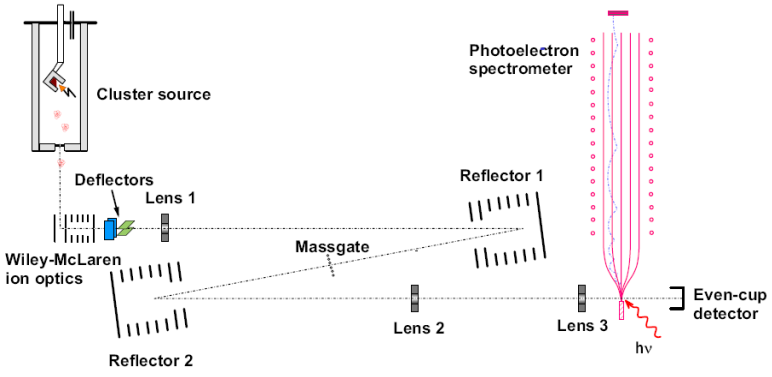

O. Kostko, PhD Thesis Freiburg 2007

Cluster stability: atomic and electronic shells

Cluster stability – ”magic numbers”

Sodium

Knight et al, Phys. Rev. Lett. 52, 2141 (1984)

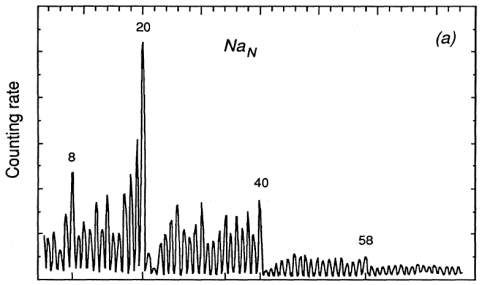

Aluminium

Martin, Phys. Rep. 273, 199 (1996)

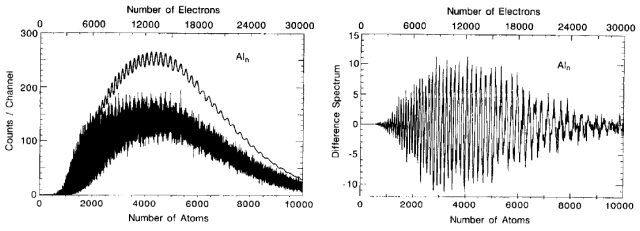

Cluster stability – atomic shells

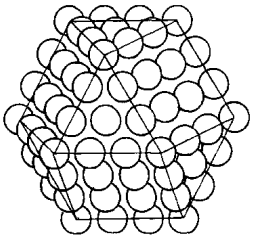

Cuboctahedron (fcc)

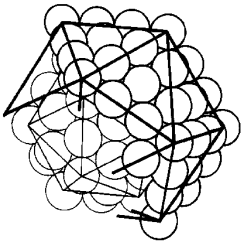

Icosahedron

T.P. Martin
Physics Reports
273, 199 (1996)

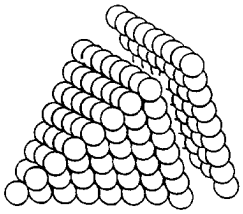

Tetrahedron (fcc)

Delocalized-electron shell model
Spherical clusters

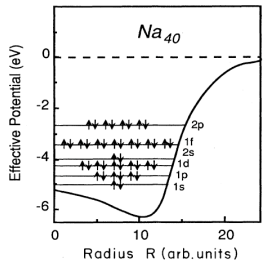

FIG. 3. Self-consistent effective potential of jellium sphere corresponding to Na_{40} with the electron occupation of the energy levels. After Chou *et al.*, 1984.

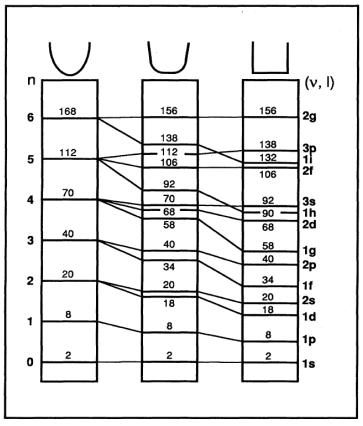

FIG. 2. Energy-level occupations for spherical three-dimensional, harmonic, intermediate, and square-well potentials. After Mayer and Jensen, 1955.

3D isotropic anharmonic oscillator

- Single-particle Hamiltonian

$$H = \frac{\mathbf{p}^2}{2m} + \frac{m\omega_0^2\mathbf{q}^2}{2} - Uh\omega_0[l^2 - n(n+3)/6]$$

$$R_0 = r_s N^{1/3} \qquad \hbar\omega_0 = E_F / N^{1/3}$$

- Eigenvalue spectrum

$$E_n = h\omega_0\{(n+\tfrac{3}{2}) - U[l^2 - n(n+3)/6]$$

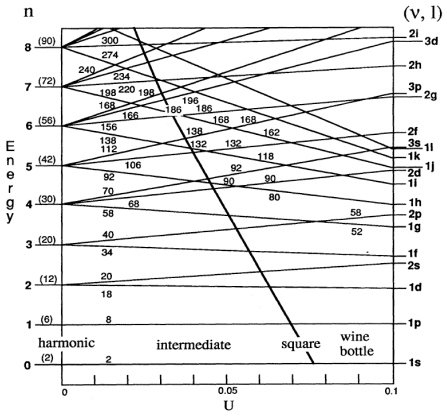

Electron shells - Effect of deformations

- Clemenger (1985) <- Nilsson (nuclear physics, 1955 !) model: for a fixed volume, the cluster shape adjusts to minimize the total energy
- Deformation → cluster radii Rx, Ry, Rz → tri-axial oscillator

$$E(n_x,n_y,n_z) = h\omega_0\left[(n_x+\tfrac{1}{2})\frac{R_0}{R_x} + (n_y+\tfrac{1}{2})\frac{R_0}{R_y} + (n_z+\tfrac{1}{2})\frac{R_0}{R_z}\right]$$

- Spheroid (Rx = Ry), distortion parameter

$$\eta = 2\frac{R_z - R_x}{R_z + R_x}$$

- Total energy for spheroids

$$E_{\mathrm{tot}}(\eta,N) = \tfrac{3}{4}\sum E(\eta,n_x,n_y,n_z)$$

Clemenger – Nilsson diagram

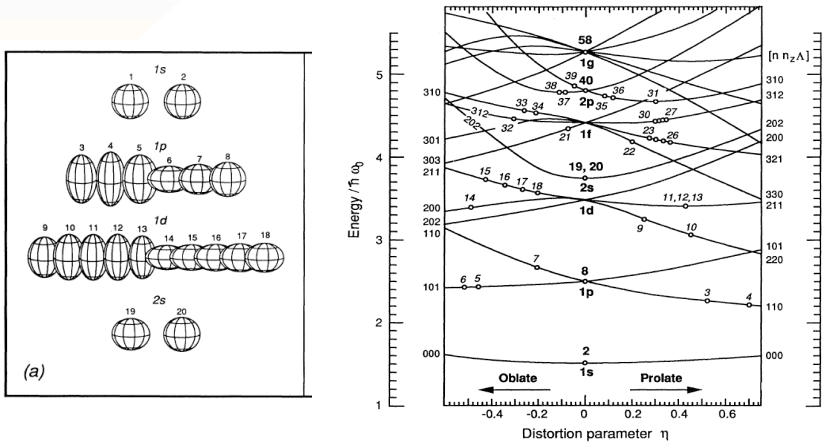

Cluster stability – electron shells

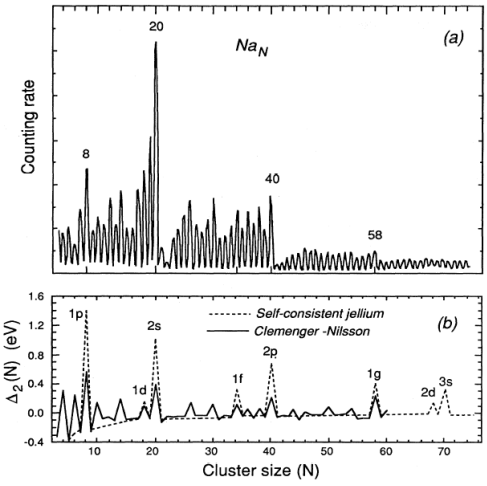

FIG. 1. Sodium cluster abundance spectrum: (a) experimental (after Knight *et al.*, 1984); (b) dashed line, using Woods-Saxon potential (after Knight *et al.*, 1984); solid line, using the ellipsoidal shell (Clemenger-Nilsson) model (after de Heer, Knight, Chou, and Cohen, 1987).

W.A. deHeer
Rev. Mod. Phys
65, 611 (1993)

Spectroscopy

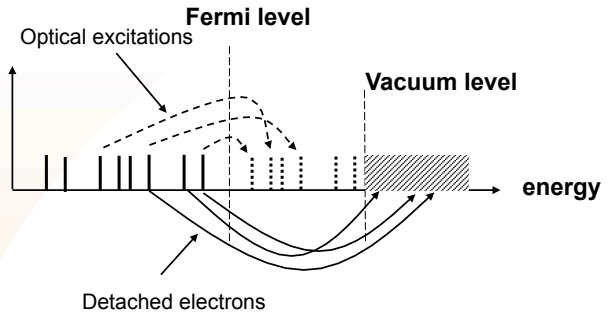

Photoabsorption spectroscopy detects the joint density of occupied and unoccupied states

Photoemission spectroscopy detects the occupied states

In the simplest approximation the spectrum is proportional to the density of states of the filled levels

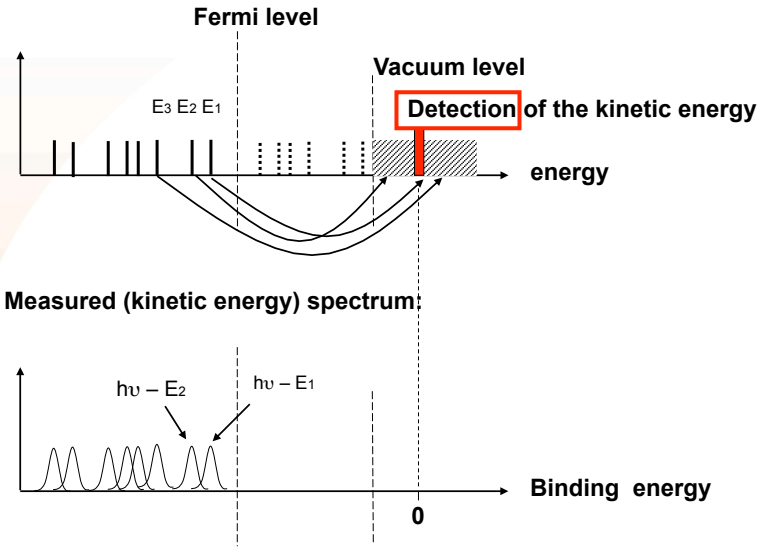

QUANTUM-SIZE EFFECTS (QSE) IN METALLIC NANOPARTICLES ?

Free-electron model of metal : density of electron states $D(\varepsilon) \propto \sqrt{\varepsilon}$

Mean spacing of electron levels at the Fermi level ε_F:

$\delta(\varepsilon_F) = 1 / D(\varepsilon_F) \sim 2\,\varepsilon_F / 3\,N\,z$ (N = number of atoms, z = valence number)

QSE observable when $\delta > kT$ (kT = 0.025 eV at 300 K)

E.g: for Au, $\varepsilon_F = 5.5$ eV, $z = 1$ →

$\delta > kT$ when $N < 150$ atoms → diameter < 1.7 nm

QSE → stabilization of the nanoparticle structure by electronic effects
→ opening of the energy gap at the Fermi level (HOMO-LUMO gap)
→ "metallic" → "semiconductor" behaviour

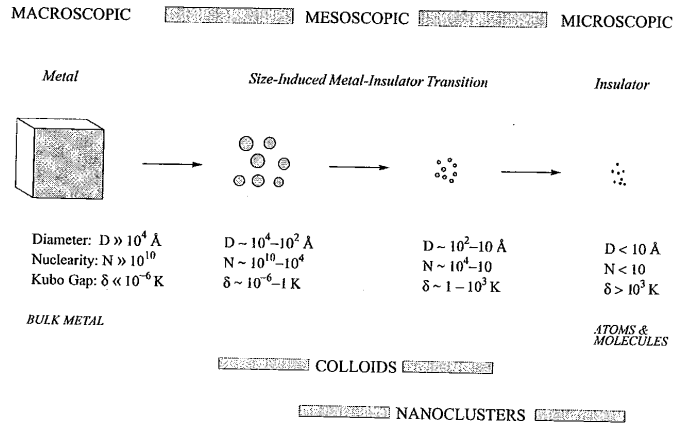

Figure 5.5 A representation of the successive division of a single grain of metal, leading eventually to a size-induced metal-insulator transition. The particle diameter (D), nuclearity (N) and Kubo gap (δ) are indicated, as are the size regimes spanned by metal clusters.

Johnston: Atomic and molecular clusters (Taylor&Francis 2002)

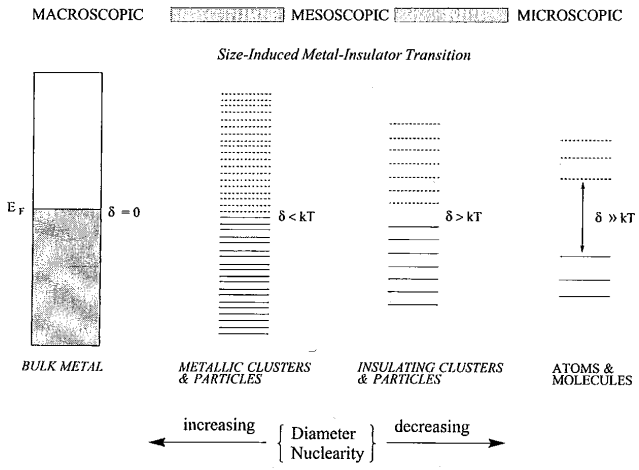

Figure 5.6 The effect of decreasing particle size (nuclearity) on the electronic structure of a metal. For finite metal particles, a Kubo energy gap opens up.

Johnston: Atomic and molecular clusters (Taylor&Francis 2002)

Experiment vs. theory: Na clusters from 4 to 350 atoms

Na cluster anions I : optimised structures at T=0 from density functional theory (DFT)

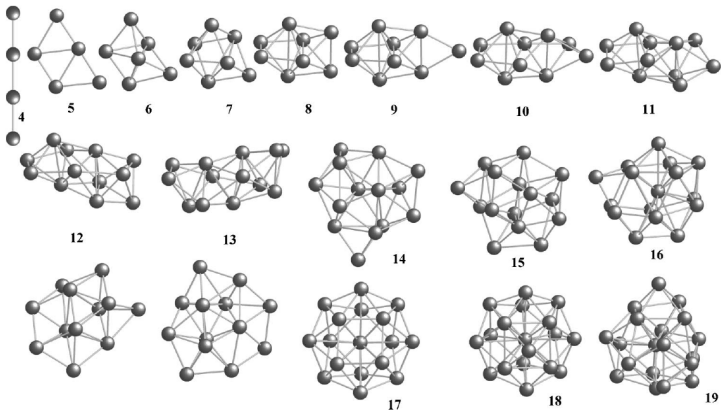

Moseler, Huber, Häkkinen, Landman, Wrigge, Hoffman, von Issendorff, PRB **68**, 165413 (2003)

Na cluster anions II : Cluster shapes from DFT

Cluster radii from GS (T=0)

Radii from RT DFT-MD

Radii from jellium model
Koskinen, Lipas, Manninen
Z. Phys. D 35, 285 (1995)

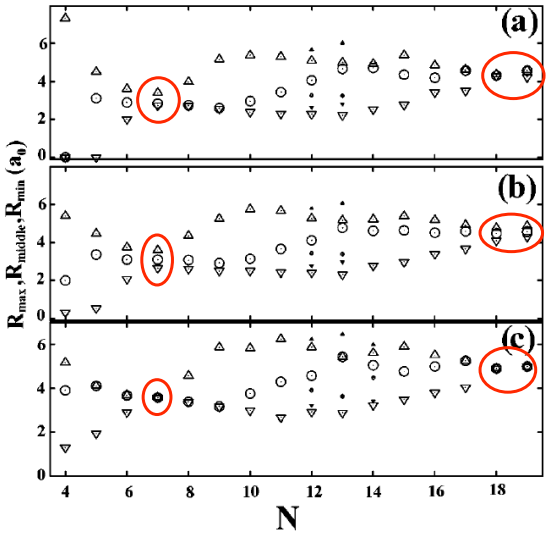

Na cluster anions III : Photoelectron spectroscopy vs. electron density of states

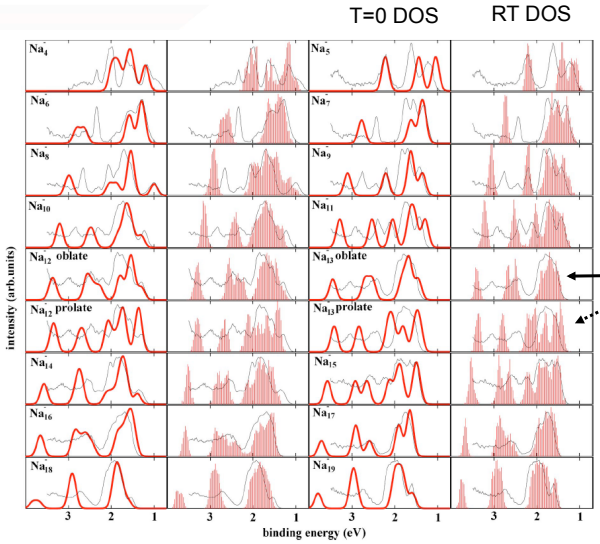

Na cluster anions IV : Photoelectron spectroscopy vs. electron density of states

55 –> 147 -> 309:

Icosahedral growth via overlayers

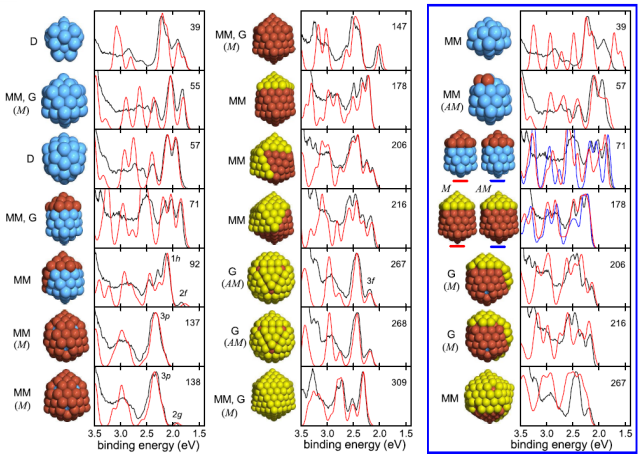

Kostko, Huber, Moseler, Issendorff, PRL **98**, 043401 (2007)

FIG. 2 (color online). Comparison of photoelectron spectra (black lines) to calculated electron densities of states (colored or shaded lines). The Kohn-Sham levels as obtained by DFT have been broadened by 70 meV width Gaussians and shifted as to reproduce the calculated electron affinity. The structures used in the calculations are indicated (left and center column: assigned ground state structures; right column: wrong structure candidates). The letters give the origin of the structures (MM: ground state structure for Murrell-Mottram potential [26], G: ground state for Gupta potential [26], D: ground state only within DFT) and indicate the structural motif of closed and open shell icosahedral structures (M/AM: Mackay/anti-Mackay overlayer [29]).